Figure 5(c), unwanted spurious resonances appear at 4.7 and 8.9 GHz because the electric lengths θ_{ia} and θ_{ib} are not exactly the same.

4. CONCLUSION

A new structure of dual-band bandpass filter has been studied in this letter. This dual-band filter with the capability of high integration and small size is very suitable for implementation in a multi-chip module. Multiple stepped impedance resonators are shunt-connected with the transmission line section. By using this approach, a transmission zero will easily appear in the middle of two passbands to increase the isolation. Our proposed technique makes it easy to design the dual-band bandpass filter with equalized bandwidth. The LTCC dual-band bandpass filters are designed and measured in frequency bands of 2 and 7 GHz. When realizing a physical 3D circuit, the parasitic effect among capacitors may cause this model to differ from the ideal values provided by the circuit simulator. These effects may make the measured and theoretical predicted results different as well. The design procedures have been described in detail, and the 3D architecture is provided. The dual-band filter has been successfully designed, and its measured results have shown good agreement with the theoretical predictions.

ACKNOWLEDGMENT

This work was supported by the National Science Council, R.O.C., under Grant NSC 95-2221-E-194-029.

REFERENCES

1. C. Quendo, E. Rius, and C. Person, An original topology of dual-band filter with transmission zeros, In: Microwave Symposium Digest, 2003 IEEE MTT-S International, Philadelphia, PA, June 8–13, 2003, pp. 1093-1096.
2. C.M. Tsai, H.M. Lee, and C.C. Tsai, Planar filter design with fully controllable second passband, IEEE Trans Microwave Theory Tech 53 (2005), 3429-3439.
3. J. Lee, M.S. Uhm, and I.B. Yom, A dual-passband filter of canonical structure for satellite applications, IEEE Microwave Wireless Components Lett 14 (2004), 271-273.
4. C.C. Chen, Dual-band bandpass filter using coupled resonator pairs, IEEE Microwave Wireless Components Lett 15 (2005), 259-261.
5. G.L. Matthael, L. Young, and E.M. Jones, Microwave filters, impedance-matching network, and coupling structures, Artech House, Norwood, MA, 1980.
6. J.S.G. Hong and M.J. Lancaster, Microstrip filters for RF/microwave applications, Wiley, New York, NY, 2001.

MEASUREMENTS OF UWB THROUGH-THE-WALL PROPAGATION USING SPECTRUM ANALYZER AND THE HILBERT TRANSFORM

Ali Hussein Muqaibel
Electrical Engineering Department, King Fahd University of Petroleum & Minerals, P.O. Box 1734, Dhahran 31261, Saudi Arabia; corresponding author: muqaibel@kfupm.edu.sa

Received 27 June 2007

ABSTRACT: *This article presents a simplified approach for characterization of ultra wideband (UWB) through-the-wall propagation. The simplified approach requires spectrum analyzer rather than vector network analyzer. A minimum phase retrieval method based on Hilbert transform is used to retrieve the phase information. The proposed method is shown to be applicable to the insertion transfer function. While linear phase component cannot be retrieved, important factors for UWB receiver design such as group delay ripple and dispersion effect can be retrieved. In noisy channels, phase retrieval could be superior to direct phase measurements. Estimation of linear phase component can be achieved through matching the measured phase with the retrieved phase.* © 2007 Wiley Periodicals, Inc. Microwave Opt Technol Lett 50: 465–470, 2008; Published online in Wiley InterScience (www.interscience.wiley.com). DOI 10.1002/mop.23107

Key words: *UWB propagation; frequency domain measurements; Hilbert transform; minimum phase; free-space measurements; network analyzer; spectrum analyzer*

1. INTRODUCTION

Indoor wireless communication signals propagate through different media. Accurate characterization of communication links requires excellent knowledge of the material properties in the communications channel. This knowledge allows for the evaluation of the applicability of the system for the indoor environment and the system coverage. A significant amount of research work has been performed for characterization of narrowband channels [1]. Because of its different nature and bandwidth occupancy, the introduction of UWB communications [2] as an alternative indoor wireless technology has given rise to the need for more measurements in the UWB frequency range.

The unique capabilities of UWB technology make it a potential candidate for short-range multiple access indoor wireless communications applications, home-networking, and secure military applications. UWB communication can support high transmission rates, has excellent wall-penetration capabilities, and consumes very low power. Besides communication applications, UWB can also be used for range measurements. UWB receivers can measure the arrival time of transmitted pulses to within a fraction of a picosecond.

In general, UWB characterization requires the extraction of the impulse response of the channel or its equivalent transfer function. The impulse response is then used to estimate the time dispersion parameters required for simulation or receiver design. Measurements can be carried out in the time domain or in the frequency domain. The conversion from the time domain to the frequency domain or vice-versa can be accomplished by the Fourier transform or the inverse Fourier transform, respectively. If measurements are conducted carefully both domains should result in similar conclusions [3].

Channel measurements for communication applications are usually performed in the frequency domain because of the availability of the required instrumentations, the moderate cost, and the large associated dynamic range [4]. The conversion to the impulse response requires both the magnitude and the phase of the frequency-domain channel transfer function. For narrowband channel characterization, the phase data are less important because the phase can be approximated as a linear phase component. For UWB channels, however, the phase is a critical parameter and the nature of its variations with frequency over an ultra-wide bandwidth can significantly impact the time-domain response. If the delay is not constant for different frequency components, the received signal will be distorted.

Vector network analyzers (VNA) can measure both the magnitude and phase. However, accurate phase measurements in environments involving long distances or wall obstructions may not be feasible. This is because the VNA requires the received signal to be fed back for comparison with the input signal. At the upper frequency edge of the bandwidth of a UWB signal, the synchro-

nization feedback cable should be of very low loss, rendering VNA measurements very costly and difficult to handle. It is also well-known that phase measurements are quite sensitive, and, unless extreme cares are taken, *in-situ* measurements have some error which will skew the final results [4, 5]. Another difficulty is that the vector network analyzer is subject to transmitter receiver crosstalk. This crosstalk might result in precursors in the impulse response [5].

On the other hand, measurements with scalar network analyzer (SNA) can be made more easily than the corresponding VNA measurements and operating SNAs does not require highly skilled personnel [6]. However, SNAs provide magnitude information only. This has led researchers to find ways of retrieving phase information, either through additional magnitude measurements or some other techniques like the Hilbert transform also known as the cepstrum technique [4, 5]. Several direct and iterative algorithms have been proposed for the reconstruction of the phase of transfer function from its magnitude, based on the pioneering work of Fienup on iterative algorithms [7, 8].

According to [4], the idea of phase retrieval was first extended to measurement of communication channels by Donaldson et al. [5]. Spectrum analyzers with Hilbert transform technique was used for UHF 1–2.5 GHz characterization [5]. Good agreement was observed between the impulse responses calculated using Hilbert transform and magnitude of the transfer function and that measured using VNA. The idea was extended to UWB communication in [9]; however, the presented channel characterization results did not include any phase dependent parameters such as time dispersion. The authors presented only large scale parameters which depend on magnitude data [9].

A quantitative measure of signal propagation through walls may be stated by the "Insertion Transfer Function." The insertion transfer function requires both magnitude and phase data which are usually measured with the VNA. In this research we examine the possibility of assessing wall-penetration capability of the UWB signals using SNA rather than VNA. It is shown that minimum phase retrieval method can be applied to insertion transfer function measurements. It is also shown that UWB group delay ripple and time dispersion can be characterized using SNA.

In the remaining parts of this article, we describe the measurement setup and procedures. The theory of phase retrieval is then discussed. The applicability of minimum phase retrieval technique based on the Hilbert transform to UWB insertion transfer function is studied. The application to typical indoor walls is also examined.

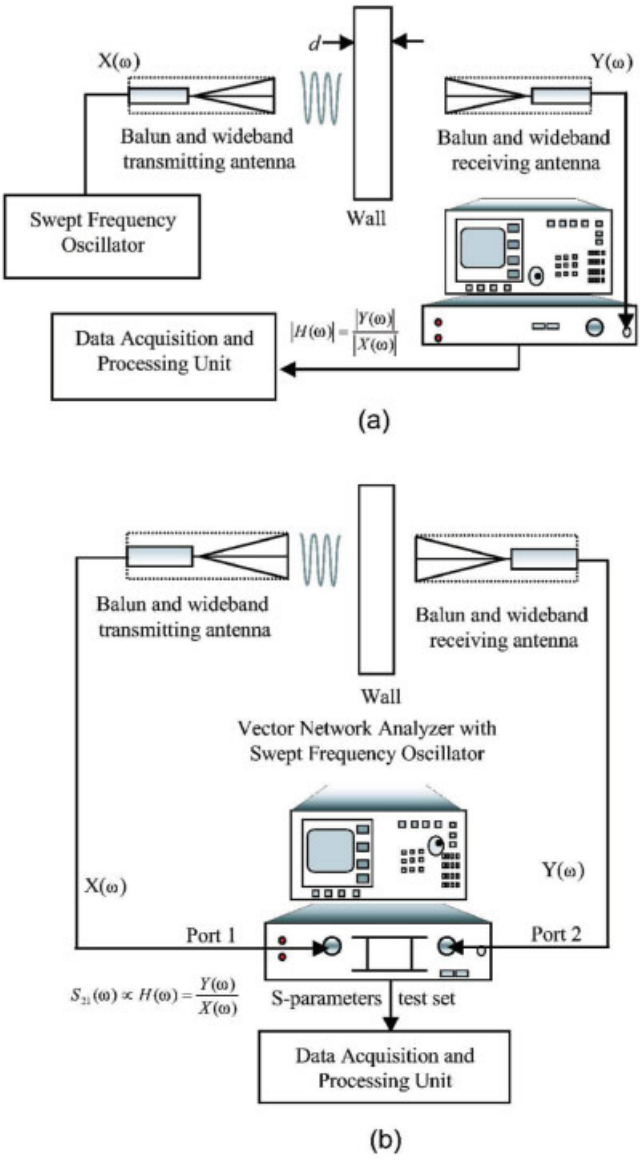

Figure 1 Measurement setup using (a) SNA, (b) VNA. [Color figure can be viewed in the online issue, which is available at www.interscience.wiley.com]

2. MEASUREMENT SETUP AND PROCEDURES

The propagation of UWB signals through different walls are evaluated through the measurement of an *insertion transfer function*, defined as the ratio of two frequency-domain signals measured in the presence and in the absence of the material slab (simulating a wall) under test. The measurements may be performed in either the time domain using short duration pulses or in the frequency domain using sinusoidal signals. Figure 1 illustrates the schematic diagram for the frequency domain measurement setup using VNA or SNA. The transmitter and receiver antennas are kept at fixed locations and aligned for maximum reception. The material to be measured is placed at nearly the midpoint between the two antennas. The distance between the antennas should be sufficiently large so that the material is in the far field of each antenna. With this arrangement, the electromagnetic field incident on the material is essentially a plane wave. The material under test is assumed to be in the form of a slab with thickness d and held in position such that the plane wave is normally incident on the slab. The main-lobe 3-dB bandwidth for the pair of TEM horn antennas used in the measurements is 1 GHz to 7 GHz. More details about the measurement setup is available in [10]. After the measurement system is prepared, initially the reference frequency-domain signal, $V^{\mathrm{fs}}(j\omega)$, is measured with a network analyzer in the absence of the material. Then, the frequency-domain signal, $V_{\mathrm{t}}(j\omega)$, is measured with the material slab in place. The insertion transfer function is calculated as

$$R(j\omega) = \frac{V(j\omega)}{V^{\mathrm{fs}}(j\omega)}, \tag{1}$$

where $\omega = 2\pi f$ is the angular frequency. It is emphasized that the measured voltages at the receiving antenna output terminals are proportional to the respective electric field intensities at the location of the receiving antenna.

Care must be taken to ensure that conditions set during the free-space measurement are as closely identical as possible to those for the measurement when the material slab is in place. It is difficult to perform *in-situ* and free-space measurements under

identical conditions. The requirement that "free-space " and "through " measurements should be performed with exactly equal antenna separations renders *in-situ* phase measurements impractical. Because, after *in-situ* "through " measurements are performed, "free-space " measurements should be carried out at a different location but with the same distance between the transmitting and receiving antennas as in the "through " measurement setup. Since it is impossible to have exactly the same distances between the antennas for measurement setups at two different locations, errors will inevitably occur in phase measurements and thus in the calculation of insertion transfer function. To emphasize how large such errors might be, a 10 GHz signal corresponding to a 3 cm free-space wavelength is considered. Only 1 mm change in the spacing between the two antennas would result in 12 degrees of phase error. This fact implies an extremely tight tolerance requirement that cannot be met easily. To overcome this problem, the phase component is dropped and a phase retrieval algorithm is used.

In this article, the VNA frequency-domain magnitude data, available from measurements in prior works [10, 11], are used. The scalar measurements considered here are not obtained using SNA but rather the measured phase information is dropped and the magnitude data for the insertion transfer function is used to obtain its phase using the Hilbert transform. In other words, the measured phase data is not utilized as was done in [10] and [11]. The theory for minimum phase retrieval will be discussed next. Because all this is based on the assumption that the impulse response is causal and analytic, this article will also assess the accuracy of the assumption to UWB radiated measurements.

3. THEORY OF PHASE RETRIEVAL

It proven in [5] that for a causal and analytical signal, $r(t)$, the real and imaginary parts of its Fourier transform denoted as $R(j\omega) = X(\omega) + jY(\omega)$, are related to each other through a Hilbert transform relationship described as $Y(\omega) = H[X(\omega)]$, hence

$$R(j\omega) = X(\omega) + jY(\omega) = X(\omega) + jH[X(\omega)], \tag{2}$$

where

$$H[X(\omega)] = -\frac{1}{\pi}\int_{-\infty}^{+\infty}\frac{X(u)}{\omega - u}du. \tag{3}$$

In many cases only the magnitude or the phase of the transfer function is known. This relation can be modified to relate the phase to the magnitude which allows for reconstruction or recovery of the unknown component [12-14]. Assuming that $r_1(t)$ is the inverse Fourier transform of $R_1(j\omega)$ given by

$$R_1(j\omega) = \ln[R(j\omega)] = \ln[|R(j\omega)|e^{j\phi(\omega)}] = \ln[|R(j\omega)|] + j\phi(j\omega), \tag{4}$$

where $R_1(j\omega)$ is a causal and analytical function, then based on (2), we have,

$$\phi(j\omega) = H[\ln[|R(j\omega)|]]. \tag{5}$$

The above relationship allows one to obtain the phase information from the magnitude information.

Measured data for $r_1(t)$ are available in discrete format, $r_1[n]$. It is necessary to measure many points in the frequency domain to make sure that the aliased version is a good approximation [4]. The integral in (3) can be interpreted as a convolution and can be implemented numerically by using the fast Fourier transform (FFT) for the sampled magnitude data produced by a scalar measurement or calculation, and by analytically solving the Fourier transform of $\frac{-1}{\pi\omega}$, to give fast compact algorithm [14]

$$\phi(\omega) = \mathrm{IFFT}\{\mathrm{FFT}(|R_1(\omega)|)\cdot(-j\cdot\mathrm{sign}(v))\}, \tag{6}$$

where v is the new transform-domain variable.

In many cases, the frequency response is known over a limited frequency range, so the derived phase function will be an equivalent minimum phase function given by:

$$H[X(\omega)] = -\frac{1}{\pi}\int_{\omega_1}^{\omega_2}\frac{X(u)}{\omega - u}du. \tag{7}$$

Since FFT is inherently periodic, some approximation has been made to the infinite integral, the error associated by periodically repeating the function must be assessed experimentally because the nature of the function is not known a priori [6].

The condition that $r_1[n]$ is causal is termed the minimum phase condition; this condition is equivalent to the situation where the Z transform of $r_1[n]$, $R_1(z)$, has no poles or zeros outside the unit circle. In general the Z transform of $r_1[n]$ sequence is expressed in a rational function form [13]

$$R_1(z) = Az^{n_0}\frac{\prod_{k=1}^{M_1}(1 - a_k z^{-1})\prod_{k=1}^{M_o}(1 - b_k z)}{\prod_{k=1}^{P_i}(1 - c_k z^{-1})\prod_{k=1}^{P_o}(1 - d_k z)}, \tag{8}$$

where M_i and P_i are the number of zeros and poles inside the unit circle, respectively, and M_o and P_o are the number of zeros and poles outside the unit circle, respectively.

The magnitudes $|a_k|,|b_k|,|c_k|$, and $|d_k|$ are less than or equal to unity, z^{n_0} is a linear phase factor, and A is a scale factor. If the response is stable, then c_k and d_k are strictly less than 1. The minimum phase condition excludes poles or zeros on or outside the unit circle in the z-plane or at infinity. Under minimum phase condition (8) reduces to

$$R_1(z) = A\frac{\prod_{k=1}^{M_1}(1 - a_k z^{-1})}{\prod_{k=1}^{P_i}(1 - c_k z^{-1})}, \tag{9}$$

where $|a_k|$ and $|c_k|$ are both strictly less than unity [13].
A necessary and sufficient condition for $r_1[n]$ to be minimum phase is that $r_1[n]$ be causal, i.e., $r_1[n] = 0, n < 0 = 0, n < 0$, and n_0 in (8) be zero which means that there is no linear phase components. The next subsection discusses the liner phase component as applied to UWB propagation then the issue of minimum phase is studied in the following subsection.

3.1. Linear Phase Component

It has to be stated clearly that the phase retrieval process cannot retrieve any linear phase component. The linear phase or the delay component cannot be recovered because it is not captured by the magnitude measurements [15]. The minimum phase function with N distinct zeros "time-domain samples" has a magnitude identical to that of $2^N - 1$ other distinct transfer functions. All of them have the same energy according to Parseval's theorem [5]. In the Z domain, replacement of zero of $R_1(j\omega)$ at z_0 inside the unit circle of the z-plane with zero at $1/z_0$ outside the unit circle leaves $|R_1(j\omega)|$ unchanged, but increases the phase delay of $R_1(j\omega)$ and also spreads the impulse response energy over time [5].

Often a priori knowledge of the linear phase factor is difficult to obtain. One possible solution in testing is to use VNA once and then use scalar network analyzer [6]. If the wall is made of well-known materials, the average relative permittivity can be used to estimate the constant delay.

While the exact delay cannot be retrieved, the group delay ripple can be extracted by differentiating the phase [14]. If the main structure of the transfer function "pass band" is contained within the measured band with a sufficiently large number of measured data, then the difference between the actual group delay of the system under test and the Hilbert-transform-derived relative group delay (HGD) will be approximately a constant across the majority of the measurement band. Large number of data means large enough to track any fast variation [6, 14].

For UWB receiver design, the group delay ripple has more significance than the constant delay as it allows for the estimation of the received pulse shape and receiver design.

3.2. Is the UWB Insertion Function Minimum Phase or Nonminimum Phase?

In general for indoor radiated channel measurements, the meaning of minimum phase is unclear [6]. According to [4], by experience, the channel behaves as a minimum phase intermittently and unpredictably, depending on the environments, frequency bands, and relative position of the antennas. No condition of the radio channel is known a priori, which allows one to state if the measurements will or will not be of minimum phase [4].

From a physical standpoint, some researchers broadly interpreted a minimum phase channel as a network with one principal signal path from the input to the output [6] and that the input arrives at the output instantaneously without a delay [15]. Based on this interpretation, most real systems are distributed and there is a delay, the Hilbert transform method is not relevant [15]. Most electromagnetic systems have a nonminimum response and the cepstrum approach given by the Hilbert Transform does not hold.

Though, the retrieval method cannot be used for the practical nonminimum phase realization which requires the function to be causal and stable and has a causal and stable inverse [16], results are still very close to exact values, For time dispersion measurements, even when the minimum phase condition is violated the calculated impulse response provides a lower bound on the time-spread of the impulse response [4].

For the insertion transfer function, the impulse response can be approximated to a single path if we assume relatively large samples and measurements are conducted in an echoic chamber. Even for indoor channels the assumption will produce relatively accurate results.

It is worth mentioning that, other nonminimum phase recovery algorithms exist. Causality can be enforced to get a unique answer for the nonminimum phase [15, 16].

4. IMPLEMENTATION AND MEASUREMENT RESULTS

In a previous work, insertion transfer function measurements on various materials commonly used in building environments were conducted. These include wooden door, glass, plywood, etc., were conducted [10]. In this article, the frequency-domain measurements is considered and the magnitude data for the insertion transfer function is used to obtain its phase using the Hilbert transform. The implementation will be illustrated for a wooden door with thickness $d = 44$ mm.

An important fact is that we are dealing with discrete data and signal conditioning is very important for proper implementation of (6). Hilbert transform can be implemented in the time domain or by utilizing FFT, do phase shift and then use IFFT. Filtering and any other signal conditioning will affect the results. A discontinuity or a sudden change of slope between the end of the data and the start of the repeated data results in a sharp change in the first derivative of the transfer function. This will cause a "ringing" effect throughout the data array after the FFT.

The use of the FFT to perform this conversion "integration" using the bandlimited measured data available is the primary

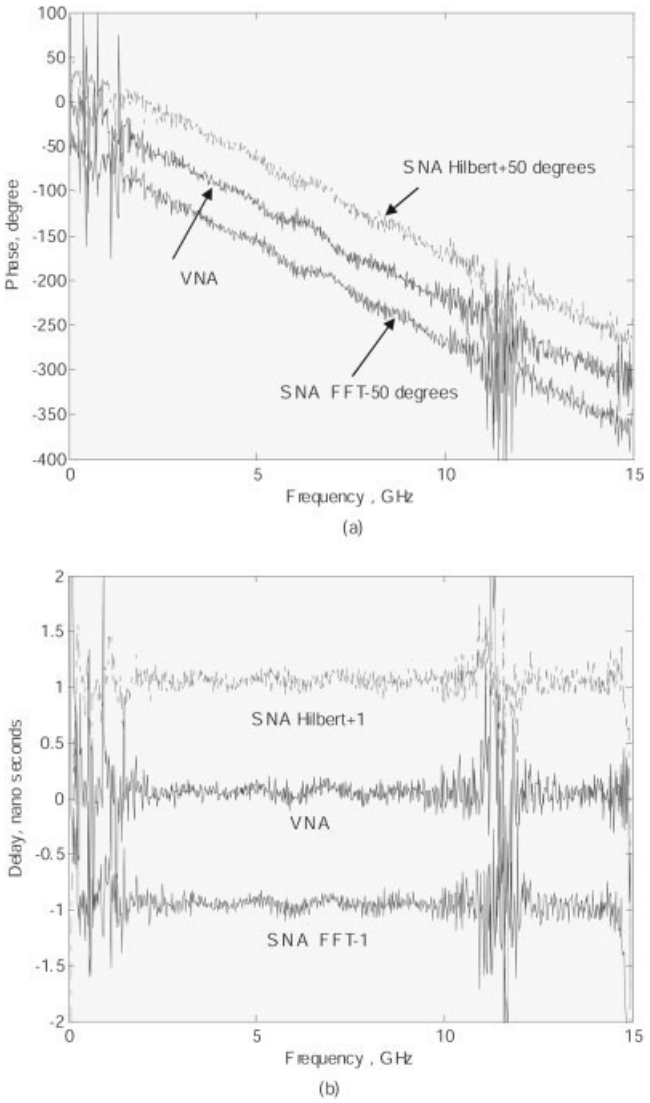

Figure 2 Phase and group delay for the Insertion transfer function with multipath components for a typical wooden door, measured using VNA and SNA (Direct Hilbert or through FFT and IFFT), (a) phase and (b) group delay

source of errors [6]. One solution is to manually adjust the data by adding few points because usually the measured data are not 2^N as required by standard FFT routines. Using interpolation function without affecting the points in the middle is also a possible remedy. Another practical solution utilizing the periodicity of FFT, to overcome the problem, the data array is doubled in size by reflecting it about the low frequency point. The first point in the FFT is forced to be real as required by the inverse Fourier transform algorithm [6].

To illustrate the effect of signal conditioning, Figure 2 depicts the phase and the group delay as retrieved by direct implementation of the Hilbert transform and as retrieved by FFT-IFFT implementation. The presented measurement is conducted in a typical indoor environment and it includes all multipath components. The magnitude results are the same. For the phase, the two methods result in excellent match with extracted phase variation. A minor difference can be observed at the noisy band between the first and second lobe of the antenna's transmission bands. The curves are shifted up and down by 50 degrees for illustration. Note that the linear phase component representing a constant delay of 0.05227 ns was manually added. The associated group delay is illustrated in part (b) of the figure. For clarity the other two curves are shifted up and down by 1 ns. Note that the average value of the VNA curve is positive representing the constant delay. Since the group delay is function of the derivative of the noisy phase measurements, a 20 points moving average is used to improve the visualization of the curves.

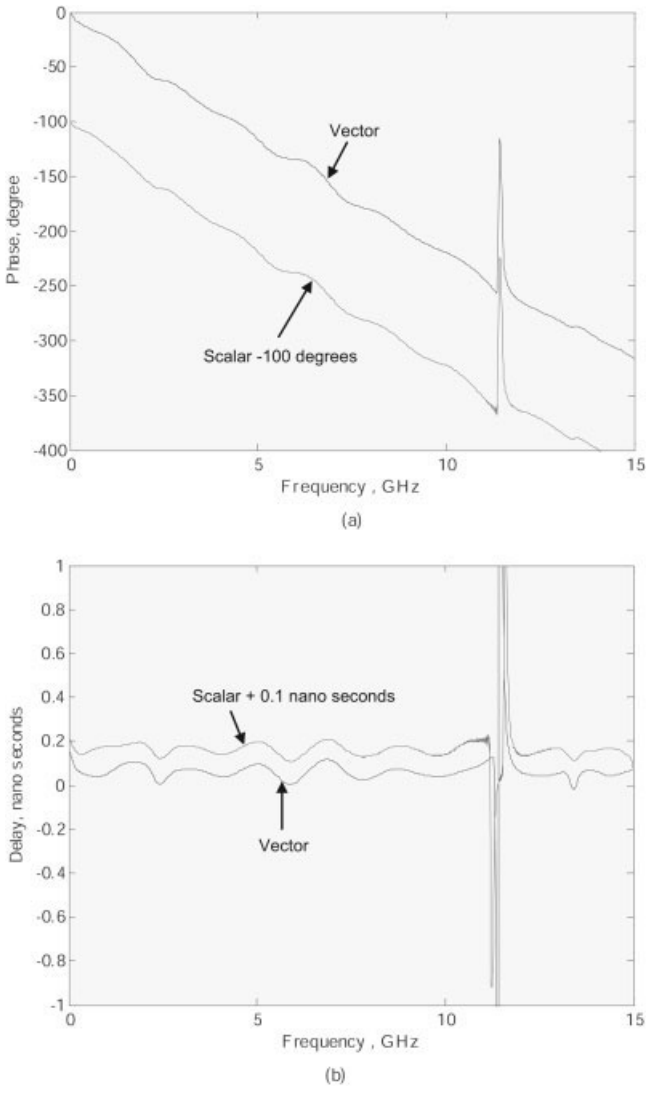

Figure 3 Phase and group delay for the insertion transfer function with no-multipath components (in echoic chamber) for a typical wooden door measured using VNA and SNA, (a) phase and (b) group delay

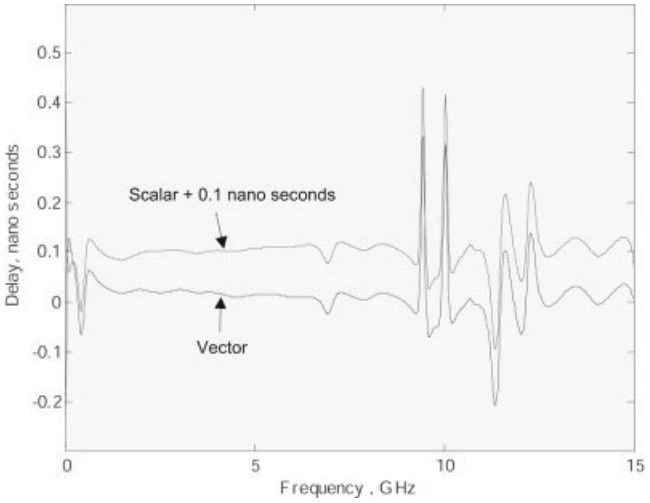

Figure 4 Group delay for the insertion transfer function through a typical glass in a controlled environment (no multipath) using VNA and SNA

As observed by [6] for other types of measurements, it is interesting to note that from the results, the VNA-based measurement becomes masked by noise when the insertion loss becomes high. The retrieved phase and group delay ripple appear to be less sensitive to measurement errors at high insertion losses.

Figure 3 illustrates the insertion transfer function with the multipath components gated out. Time gating cannot be implemented using SNA, but instead the measurement can be carried out in an echoic chamber to eliminate the reflections. Multipath components manifest themselves as a fast changing component on top of the frequency response. The extracted phase and group delay are shifted for a comparative view.

Except for the noisy band of the spectrum, we can see almost a complete retrieval of the phase and delay. Once again the linear phase component is added manually which stands for 0.059 ns different than the multipath case. In fact, matching the measured phase with the retrieved phase provides an excellent alternative for estimation of the average group delay (constant delay or linear phase components). Alternatively the constant delay could be estimated from the impulse responses.

The results where verified using a different pair of antennas and using different materials. For illustration the group delay for a typical glass used in indoor construction is depicted in Figure 4.

Principal sources of errors have been identified by [6] as two. First, errors arising from the numerical algorithm used: primarily, due to the periodic extension of the data. There is a compromise between measurement bandwidth and accuracy. The second source of errors is inherent in the scalar measurement system. In our study only the first source can be observed.

5. CONCLUSIONS

This paper validates the application of Hilbert transform-based phase retrieval method to UWB signals, thus paving the way for simpler, less expensive, and faster measurements for researchers active in the UWB field. We have shown that minimum phase retrieval method using Hilbert transform is applicable to the insertion transfer function

in controlled and non-controlled environments. This allows the use of SNAs and in-situ measurements. Although the linear phase component cannot be retrieved, important factors for UWB receiver design such as the group delay ripple and time dispersion effect can be extracted. In many potential application problems, the measured phase data may have been degraded by measurement and quantization noises. We have shown that phase retrieval could be superior to direct phase measurements for signals propagating through noisy channels. When VNA measurement is conducted, estimation of linear phase component can be achieved through matching the measured phase with retrieved phase.

ACKNOWLEDGMENTS

This work was supported by King Fahd University of Petroleum and Minerals. The author would like to thank Prof. A. Safaai-Jazi and Prof. M. Abuelma'atti for their constructive ideas and fruitful discussions.

REFERENCES

1. T.S. Rappaport, Wireless communications, Principles & Practice, Prentice Hall, Inc., 1996.
2. R.A. Scholtz, Multiple access with time-hopping impulse modulation, MILCOM 2 (1993), 447-450.
3. D. Tholl, M. Fattouche, R.J.C. Builtitude, P. Melancon, and H. Zaghloul, A comparison of two radio propagation channel impulse response determination techniques, IEEE Trans Antennas Propag 41 (1993), 515-517.
4. I. Páez, S. Loredo, L. Valle, and R. Torres, Experimental estimation of wide-band radio channel parameters with the use of spectrum analyzer and the Hilbert transform, Microwave Opt Technol Lett 34 (2002), 393-397.
5. B.P. Donaldson, M. Fattouche, and R.W. Donaldson, Characterization of in-building UHF wireless radio communication channels using spectral energy measurements, IEEE Trans Antennas Propag 44 (1996), 80-86.
6. P. Perry and T.J. Brazil, Hilbert-transform-derived relative group delay, IEEE Trans Microwave Theory Techn 45 (1997), 1214-1225.
7. J.R. Fienup, Reconstruction of an object from the modulus of its Fourier transform, Optics Lett 3 (1978), 27-29.
8. J.R. Fienup, Phase retrieved algorithms: A comparison, Appl Opt 21 (1982), 2758-2769.
9. A. Bayram, A.M. Attiya, A. Safaai-Jazi, and S.M. Riad, Frequency-domain measurement of indoor UWB propagation, IEEE Int SympAntennas Propag 2 (2004), 1303-1306.
10. A. Muqaibel, A. Safaai-Jazi, A. Attiya, B. Woerner, and S. Riad, UWB through the wall propagation, IEE Proc-Microwaves Antennas Propag 152 (2005), 581-588.
11. A. Muqaibel and A. Safaai-Jazi, A new formulation for characterization of materials based on measured transfer function, IEEE Trans Microwave Theory Tech 51 (2003), 1946-1951.
12. A. Bayram, A.M. Attiya, and A. Safaai-Jazi, Frequency-domain measurement of indoor UWB channels, Microwave Opt Technol Lett 44 (2005), 118-123.
13. T. Quatieri, and A. Oppenheim, Iterative techniques for minimum phase signal reconstruction from phase or magnitude, IEEE Trans Acoust Speech Signal Process 29 (1981), 1187-1193.
14. P. Perry and T.J. Brazil, Hilbert-transform-derived relative group delay measurement of frequency conversion systems, IEEE MTT-S Inter Microwave Symp 3 (1996), 1695-1698.
15. Jie Yang, Jinhwan Koh, and T.K. Sarkar, Reconstructing a nonminimum phase response from the far-field power pattern of an electromagnetic system, IEEE Trans Antenn Propag 53 (2005), 833-841.
16. J. Koh and T.K. Sarkar, Reconstruction of the non-minimum phase function from amplitude only data, IEEE MTT-S Int Microwave Symp 2 (2000), 1093-1096.

A CLASS-E CMOS RF POWER AMPLIFIER WITH CASCADED CLASS-D DRIVER AMPLIFIER

Jaemin Jang, Hongtak Lee, Changkun Park, Songcheol Hong
School of Electrical Engineering and Computer Science, Division of Electrical Engineering Korea Advanced Institute of Science and Technology, 373-1 Guseong-Dong, Yuseong-Gu, Daejeon 305-701, Republic of Korea; Corresponding author: suppli@kaist.ac.kr

Received 27 June 2007

ABSTRACT: *A 800-MHz power amplifier is designed using a 0.18-μm RF CMOS process. The voltage-combining method is used for power combining. A transmission line transformer on a printed circuit board (PCB) is designed as a power combiner. For the switching mode power amplifier, a cascaded class-D driver amplifier is proposed using a feedback resistor and a DC-blocking capacitor. The power amplifier has an output power of 32.9 dBm and a power-added efficiency of 60.25%.* © 2007 Wiley Periodicals, Inc. Microwave Opt Technol Lett 50: 470–473, 2008; Published online in Wiley InterScience (www.interscience.wiley.com). DOI 10.1002/mop.23106

Key words: *class-D; CMOS, driver amplifier; PCB; power amplifier; transmission line transformer*

1. INTRODUCTION

The polar transmitter is an attractive architecture for wireless communication technology, which requires high linearity and high efficiency. The polar transmitter delivers envelope information and phase information through separated paths. A simplified general polar transmitter is shown in Figure 1 [1, 2]. The envelope information of the polar transmitter is resorted by adjusting the supply voltage of the power amplifier, which has a RF phase input signal with constant amplitude. The efficiency of the power amplifier accounts for the greater part of the total efficiency of the transmitter. To improve the efficiency of the transmitter, a switching-mode power amplifier with high efficiency is used for the polar transmitter. To integrate analog circuits and digital circuits used in the polar transmitter, the power amplifier should be developed with a CMOS process. Because of low breakdown voltage and poor passive devices in CMOS processes, however, designing a CMOS power amplifier with high output power, efficiency, and linearity poses a considerable challenge [3, 4].

Recent study has shown the possibility of utilizing CMOS technology for switching-mode power amplifiers [3, 4]. However, it is difficult to realize a passive device with a high-quality factor due to the lossy silicon substrate of the CMOS process. In a previous work [5], a voltage-combining technique with a printed circuit board (PCB) transmission line transformer was realized. And obstacles to the design of a watt-level CMOS power amplifier were overcome. In this work, a voltage-combining technique with a PCB transmission line transformer is used. Additionally, a

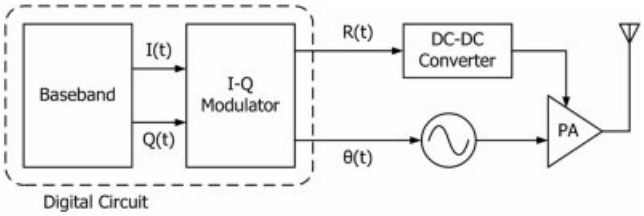

Figure 1 Block diagram of polar transmitter